The International Journal of Advanced Manufacturing Technology
https://doi.org/10.1007/s00170-021-06891-0

ORIGINAL ARTICLE

A hybrid additive manufacturing platform based on fused filament fabrication and direct ink writing techniques for multi-material 3D printing

Thibaut Cadiou[1] · **Frédéric Demoly**[1] · **Samuel Gomes**[1]

Received: 25 November 2020 / Accepted: 9 March 2021
© The Author(s), under exclusive licence to Springer-Verlag London Ltd., part of Springer Nature 2021

Abstract
Among the available additive manufacturing (AM) technologies, fused filament fabrication (FFF) technique—broadly used in academia—seems to be a promising alternative to injection molding process in industry regarding physical prototypes. This is partially due to its accessibility, fast responsiveness and the substantial development of low-cost and open-source machines and filament materials. However, beyond the ongoing research efforts related to this material extrusion technique, the inherent layer-by-layer deposition strategy leads to lower mechanical performances compared to traditional formative and subtractive manufacturing processes. Indeed, recurrent anisotropic material properties and fracture strength still remains as the key challenges to be tackled in FFF, so as to get close to mechanical performances obtained by injection molding. In such a context, the main objective of the article is to extend mechanical parts' performances by improving fracture strength of FFF printed parts. To do so, an innovative hybrid additive manufacturing platform—combining FFF and direct ink writing (DIW) techniques—is proposed. The proposed platform is implemented through a dedicated digital workflow covering process planning algorithms and a new modular concept of hybrid 3D printer. The added value of the proposal is demonstrated with tensile strength tests and opens the door to multi-material 3D printing.

Keywords Additive manufacturing · Fused filament fabrication · Direct ink writing · Hybrid additive manufacturing

1 Introduction

Additive manufacturing (AM) can be seen as a revolutionary and promising technology to build prototypes, assemblies or parts in small series production [1–3]. Beyond the numerous advantages provided by this manufacturing technology, some barriers still remain to be solved as the low mechanical behavior (i.e. tensile strength, Young's modulus, elongation at break) compared to injection molding (IM) [4].

The adoption of such a manufacturing paradigm in industry is therefore a key competitive challenge whether for building functional prototypes, customized parts or mass-produced ones. In such a context, this paper proposes to address scientific and industrial needs on rapid prototyping of plastic parts. This is more particularly expected in automotive industry, for which plastic prototypes are usually built to evaluate and check the design solution from an assembly point of view. Once done, injection molds are then designed and fabricated for mass production purposes. In order to make right decision regarding the life cycle evaluation of the physical prototype, it becomes critical to build more realistic and fidelic prototypes—in terms of mechanical behavior compared to final manufactured parts—at lower cost with fast respond on demand. Among the available AM processes and techniques, fused filament fabrication (FFF) technique seems to be quite appropriate to build plastic physical prototypes at lower cost [5, 6]. This layer-by-layer deposition technique is now well democratized and has received tremendous attention from filament manufacturers in order to print parts from wide spectrum of materials. Although FFF technique is suitable to print 3D parts with various kinds of material, it exhibits limitations which need to be solved.

Literature has highlighted the difference between parts made with FFF techniques and IM in terms of anisotropic behavior and low tensile strength at break [7, 8]. FFF techniques actually present not only advantages in building

✉ Frédéric Demoly
frederic.demoly@utbm.fr

[1] ICB UMR 6303 CNRS, Univ. Bourgogne Franche-Comté, UTBM, Belfort, France

Published online: 28 April 2021

quickly physical prototypes but also weaknesses in mechanical behavior that could potentially be a barrier for an industrial adoption [4, 9, 10]. Among the efforts made in this research direction, several works have studied the influence of the process parameters—such as raster orientation, air gap, bead width, colours and bed temperature—on the anisotropic behavior of ABS materials, resulting in an ultimate tensile strength at break (UTS) between 65 and 72% compared to IM [7, 11, 12]. By considering the same materials, Zhang et al. [13, 14] have highlighted the part distortion related to mechanical loads, thermal phenomena and phase transition temperature. They have also shown the influence of the printing paths on part distortion, leading to better properties when long paths are applied since short paths infer more residual stress. In addition, Alaimo et al. [15] have studied how dimensions and chemical composition can impact the parts' mechanical properties. In a similar way, Li et al. [16] have emphasized that a perfect cohesion between two deposited beads—leading to an isotropic behavior—could only be achieved via a room temperature above the glass transition temperature. Such claim is however not achievable due to the caused material distortion over the glass transition temperature. Recently, Li et al. [16] have evaluated the residual stress of a 3D printed part using FFF technique regarding the cohesive zone between two layers in contact and have stated that strong mechanical parts with the least deformation require the biggest layer thickness that could be a contradiction with the industrial need in high printing resolution.

From a simulation perspective, Martinez and al. [17] have carried out research with finite element method to simulate the mechanical behavior of FFF printed parts, therefore demonstrating that the FFF parts were orthotropic as composite parts. For such composite parts, Zhao and al. [18] have created a model to predict the Young modulus and the UTS for PLA parts regarding few parameters such as layer thickness and raster orientation with less than 14% error. For instance, this could help to predict simple mechanical phenomena such as uniaxial stress or plane stress. All these aforementioned studies have highlighted the lack of solutions for improving capabilities of FFF technique in order to build plastic parts with similar mechanical properties compared to IM.

To overcome this issue, researchers have addressed hybrid techniques combining resins and filaments. As such, Zaldivar et al. [19] have manually filled epoxy resin into ABS parts build with a Fortus 250 mc machine in order to strengthen ABS parts. Other researchers have developed open-source resin extruders—such as Ystruder [20] and Fab@home projects [21]—to infill FFF printed parts. Such projects have introduced the direct ink writing (DIW) technique which not only presents great flexibility but also lacks of versatility. On the other hand, Wang et al. [22] have developed a versatile and modular 3D printer called xPrint that enables the deposition of various liquid viscosities including inks and hydrogels. Although the developed system is limited to liquids, it could be used to build a mold with hydrogel for further resin deposition. Similarly, the fact of infilling FFF printed parts with resins has already been tackled and successfully achieved via chemically hardening polyurethane but suffers from a lack of automation [23, 24]. These works have improved mechanical behavior of hybrid manufactured plastic parts compared to specimens only built with FFF technique and 100% ABS material. To increase the parts' mechanical performances, one can state that most of the research works have been focused on the optimization of process parameters. However, the resulted optimized parameters configurations still do not enable to build plastic parts as strong as those made with IM.

Based on this aforementioned study—which has highlighted the current status and challenges towards building plastic parts with improved mechanical behavior—the main objective is then to develop a hybrid AM technique combining FFF and DIW advantages in a single build with automation procedures [25, 26]. Such a hybrid technique aims at building the part's shell (i.e. the external skin of the part's body) and the part's infill (i.e. the part's body). The structure of the paper is as follows. Section 2 presents an innovative hybrid additive manufacturing platform in terms of design principles, geometric definition, hardware composition and process planning algorithms. Section 3 conducts experimental tests built from a customized hybrid 3D printer prototype and open the door for discussions and future work.

2 Hybrid AM platform overview

This section presents the proposed hybrid AM technique and its implementation in terms of machine design and digital workflow integrating process planning algorithms.

2.1 Working scenario

Actually fabricating composite parts in a single build with FFF and DIW techniques leads to consider both layer-by-layer and volume-by-volume deposition strategies. In such a context, composite components can be decomposed in shell and infill parts, thus processed by FFF and DIW techniques respectively.

Here, the research hypothesis is to build composite parts with better mechanical behavior than 100% FFF manufactured parts behavior. As functional requirement, an

original working scenario—illustrated in Fig. 1—has been set up and defined as follows:

1. The shell part is built by only using FFF technique. In this step, additional aids—such as bed adhesion and cantilevered parts support—are also considered. The filament deposition stops before closing the shell, therefore leaving the resin infill step.
2. Once the open shell is built, the resin infill is processed by DIW and gravity in a volume-by-volume manner. In this step, time saving is ensured since no path planning is needed.
3. Afterwards, the last step consists in closing the shell part with FFF technique.

With such a proposed 3D printing scenario, technical issue can arose, especially concerning the infill of parts integrating multiple closed shells. For this specific case, it is important to determine the location of closed shells and their spatial distribution over z axis in order to define an appropriate AM process plan. Indeed, complex geometric parts are needed to be broken down into multiple discrete bodies in order to properly ensure the infill step. To tackle this process planning issue regarding part's geometric complexity, new algorithms have been developed in Section 2.3 so as to analyze critical part's bodies and then define separate infill steps in an efficient manner.

2.2 Hybrid 3D printer development

The proposed system architecture—where its detailed design is illustrated in Fig. 2—is similar to an open source CNC machine, on which additional modules have been allocated, i.e. a FFF extruder for filaments and a DIW dispenser for resins. Three translation are enabled between a heated bed and the aforementioned extrusion modules. More exactly, x and z axis translations are allowed by the printing heads, both of them independently move in the x direction and have a dependent displacement in the z direction. The last degree of freedom is enabled by the heated bed. The printing heads have been attached to the printer chassis by following feeding mechanisms like Bowden extruder [27], pushing filaments and resins through a long and flexible polytetrafluoroethylene (PTFE) tube to the heads, and therefore reducing the mass of extrusion carriage. For further details on the bill of materials, please refer to Appendix.

2.2.1 Structure

The developed hybrid 3D printer is a retrofit of an Anet A8 low-cost 3D printer with an customized chassis made of aluminium profile frames. The use of low-cost printer components make it affordable and still provide enough accuracy and repeatability to serial prototyping. Here, all the interface parts between the various low-cost printer components and the off-the-shell extruder components (see Fig. 2) have been additively manufactured by using a FFF 3D printer. The displacements resolution of the heated bed is defined at 10 µm and 2.5 µm for printing heads. The heated bed has a printing area of 220 mm × 220 mm. The z-motion movement is only 150 mm but can be easily changed by changing the length of four aluminium profiles and two trapezoidal screws. All the guidance systems are 8-mm rods commonly used in the 3D printing community. Figure 3 gives an overview of the customized hybrid AM platform. In the present work, the accuracy has not been improved. The proposed hybrid AM platform offers accuracy similar to traditional FFF 3D printers.

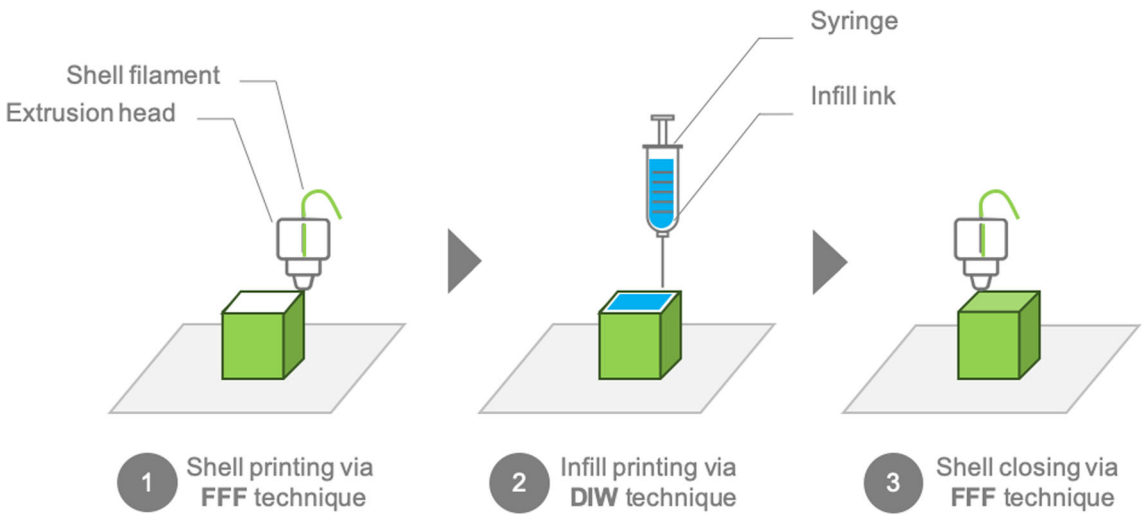

Fig. 1 Proposed concept of hybrid additive manufacturing technique

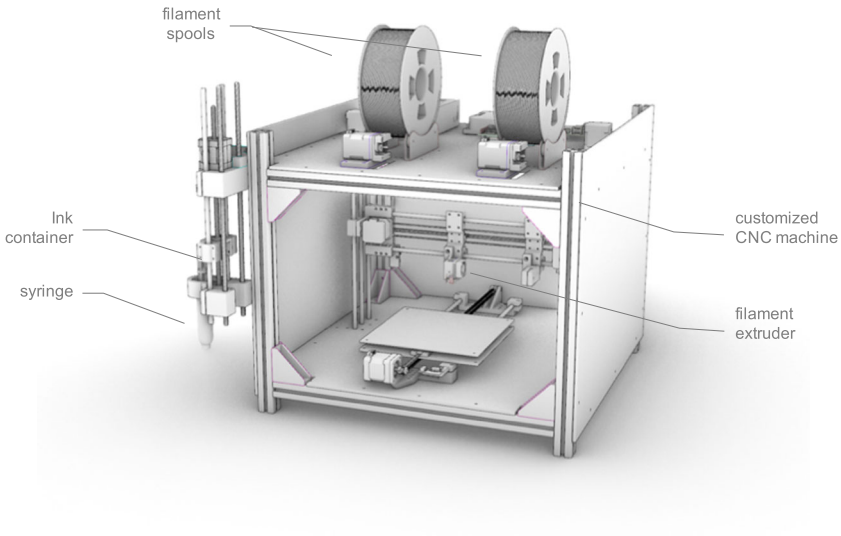

Fig. 2 Detailed design of the proposed hybrid 3D printer

2.2.2 FFF module

The FFF extrusion module used is a Chimera head [28], which allows to print in a same build compatible structural and sacrificial materials based on polymer like polylactic acid (PLA)/polyvinyl alcohol (PVA) and acrylonitrile butadiene styrene (ABS)/high-impact polystyren (HIPS). The Chimera head is composed by two inputs/outputs for depositing two different 1.75-mm diameter filaments. The extruder has been allocated as a Bowden system enabling the control of the filament flow from the printer chassis.

2.2.3 DIW module

The DIW module is composed of a 30-cc syringe barrel as resin container, a tube (not represented in Fig. 2) ensuring the connection between the DIW dispenser and the needle. A stepper motor working with a trapezoidal screw is used to actuate the appropriate resin flow. This dispenser has a deposition volume resolution as follows (Eq 1):

$$V = \frac{\pi \times d^2}{4} \frac{n \times p}{Ns \times m} = \frac{\pi \times 21.53^2}{4} \frac{4 \times 2}{200 \times 16} = 0.910\, mm^3 \quad (1)$$

where V is the minimum deposition volume (in mm^3); d is the diameter of the inside of the syringe (in mm); n stands for the number of threads of the spindle; p represents the thread pitch (in mm); Ns is the motor microstep number per revolution; and m means the number of microsteps. Similar to the FFF extruder, this resin dispenser requires a reliable procedure. It firstly consists in filling the syringe barrel and the tube channeling the resin to the mobile needle. During this stage, the tube end is locked so as to control resin flow. Once the DIW module filled, the piston is introduced to provide a controlled resin pressure. Afterwards, trapped air

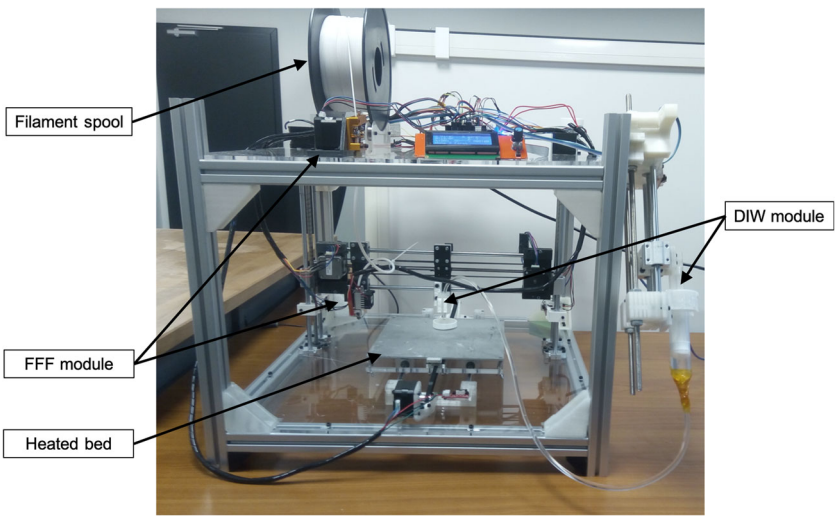

Fig. 3 Realized hybrid 3D printer

within the system is removed by unlocking the needle and then purging few resin.

2.2.4 Electrical control

The printed circuit board used to control the machine is built upon an Arduino 2560 uno Rev 3 and a Ramps 1.4, therefore enabling to drive up five stepper motors, i.e. DC motors able to move in discrete steps. However, the design decisions regarding printer architecture have raised the need to use seven stepper motors to fully control the three stages of the proposed hybrid AM technique. To cover this additional requirement, few electronic extensions have been incorporated to control the second x and z axes. Acting as a communication channel, a RepRap Smart Controller has been implemented so as to control the resin flow in the DIW dispenser [29]. By using such a communication protocol, the printer can work in a standalone way. It should be noted that all these aforementioned components are open source and well documented, which make the system quite versatile to any kind of deposition requirement.

2.2.5 Firmware

Based on these mechanical and electronic solutions, a firmware—built upon Marlin [30]—has been implemented in order to control the hybrid 3D printer. Actually, Marlin firmware is enough suitable to control multiple extrusion modules; however, changes have been made to consider the control of additional stepper motors. Such changes concern the use of available general-purpose input and output (GPIO) of the microcontroller in order to implement two stepper motors, i.e. one enabling the DIW dispenser move along x axis and another for the DiW needle z axis displacement. Such configuration ensures the independent move of the DIW needle in relation to the FFF printhead. Moreover, some adaptations were also made to have an asynchronous behavior of the two z stepper motors during the reference travel along the z axis. As a result, all these settings ensure a better repeatability of the parallelism between the heated bed and the x axis.

2.3 Process planning

The setup of such innovative AM platform also requires an appropriate digital workflow in order to push any 3D models to physical reality. To do so, a set of softwares and algorithms have been specified for converting 3D design models in terms of volumes, shells, bodies and finally printing paths into G-code instructions. Such a digital workflow highlights the need to integrate a reasoning layer in order to define proper an AM process plan combining FFF and DIW instructions. The proposed flowchart—illustrated in Fig. 4—is based on three novel algorithms dedicated to allocate the right AM strategy (i.e. layer-by-layer or volume-by-volume) to the right geometry part at the right time.

The objective here is to build the part shells by using FFF technique in a layer-by-layer manner, and also the inner volume with the DIW technique in a volume-by-volume strategy. Therefore, the Algorithm 1 aims at scanning the 3D model of the part along the z axis from the initial layer height h_0 to the final one h_f in order to identify closed volumes. This means that the process planner has to properly define the printing position and orientation of the part beforehand. For each identified closed volume, the Algorithm 2 is carried out to slice it (i.e determining the printing paths on a specific z layer) and then to generate the G-code instructions. Afterwards, the last Algorithm 3 is applied to concatenate and sort out all G-code instructions.

Algorithm 1 Closed volume(s) identification.

```
Input:
Layer height
set of processed and unprocessed closed surfaces
set of closed volumes
Output:
new set of processed and unprocessed closed surfaces
new set of closed volumes

Find the edges at the intersection between the model
and the XY plane at layer height
Deduce the closed surfaces to print
foreach closed surfaces to print do
    Number of anteriority for the closed surface to
    print with the surfaces to print of the previous layer
    if Number of anteriority equal to 0 then
        The layer height is the start of a new volume
        Attribute an indice to the new volume
        Attribute the closed surface to print to the new
        set
    else if Number of anteriority equal to 1 then
        Attribute the closed surface to print to the same
        set as the close surface to print of the previous
        layer
    else if Number of anteriority superior to 1 then
        The layer height is the start of a new closed
        volume
        Attribute an indice to the new volume
        Close the anterior sets
end
Update the set of processed and unprocessed closed
surfaces
Update the set of closed volumes
Return G-code instructions
```

Algorithm 2 Volume(s) slicing.

Input: Closed volume(s) not yet sliced
Output: Closed volume(s) sliced and its associated G-code instructions

set the initial layer height and the final layer height
set the layer height equal to the initial layer height
set the volume of resin to 0
set boolean *isDIWDone* to false
while *the layer height hasn't reach the final layer height* **do**
  if *the layer height is inferior to the shell's bottom thickness* **then**
    Create G-code for bottom
  else if *the layer height is inferior to the final layer height minus the shell's top thickness* **then**
    The volume of resin equal the previous volume of resin plus the layer height times the inner area of the closed surface
    Create the shell's G-code
  else
    if *isDIWDone is false* **then**
      Create G-code for DIW
      set *isDIWDone* to true
      Create shell's top shell G-code
    end
    Create shell's top shell G-code
  end
end
Return Closed volume(s) sliced and its associated G-code instructions

Algorithm 3 Concatenation of G-code instructions.

Input: the set with all the G-code instructions
Output: the final G-code for the printing of the whole geometry

Concatenate all G-codes instructions
Sort by z height
foreach *z height* **do**
  Put the DIW's related G-code
  Then FFF's G-code
end
Assemble the intial and the final G-code to the sorted G-code
Return The G-code ready to print

The aforementioned process planning algorithms are currently implementing—using Python scripts—within Rhinoceros 3D environment and its dedicated visual programming plugin, Grasshopper. The latter enables the development of specific programs and promotes parametric and flow-based 3D part definition. Figure 5 illustrates the dedicated Grasshopper workflow enabling the interpretation of any 3D models in terms of closed volumes, the computation of AM technique instructions and concatenation into a single G-code file.

3 Results and discussions

3.1 Experimental protocol for testing mechanical behavior

To demonstrate the usefulness of such a hybrid technique/platform, experimentations have been carried out to evaluate the mechanical performances of multi-material printed parts. Among the key performance indicators, the UTS has been considered as the main critical criteria to evaluate and compare specimens built from various manufacturing techniques and strategies. At this stage, the proposed machine is enough suitable to build specimens with the following AM strategies (see Fig. 6):

(a) Using only FFF technique for the whole part. It consists in vertically printing the specimen along its length with PLA 4043D material [31] and 100% infill.
(b) Using FFF technique for shell printing and DIW for infilling the part as highlighted in Section 2. Related specimens have been built with PLA 4043D as FFF material and epoxy resin SR GreenPoxy 56 with an hardener SD 7561 as DIW material. The ratio of resin in the cross section is 65% for the 22.5mm^2 specimens, 74% for the 45mm^2 specimens and 80% for the 67.5mm^2 specimens;
(c) Using FFF technique to print a sacrificial PVA mold and then infilling it with the DIW dispenser. Related specimens have been built with the epoxy resin SR GreenPoxy 56 and an hardener SD 7561.

The material used for those specimens and the main process parameters for the FFF technique are shown respectively in Tables 1 and 2.

As an evaluation reference, IM is also used to build specimens made of PLA pellets 4030D in order to provide the theoretical maximum UTS to be targeted for isotropic parts. The IM process has been carried out by setting up an injection pressure of 700 bars, an extrusion flow of 24 cm s^{-1} and an injection temperature of 200°C. To properly evaluate specimens' mechanical behavior, the theoretical UTS needs to be considered with a mixing law applied to a composite material as defined in Eq. 2, where σ_{eq}

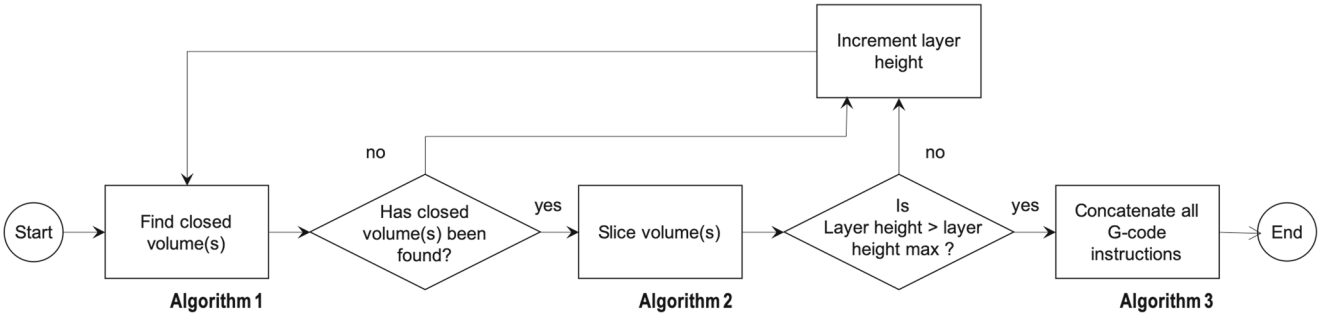

Fig. 4 Flowchart of the proposed process planning

stands for the maximum UTS of the composite part, σ_{DIW} represents the maximum UTS of the resin, V_{DiW} the ratio of resin in the cross section and σ_{FFF} the maximum UTS of the FFF material. As such, the UTS can be determined regarding the plastic filament and the resin used as well as the ratio of the two materials in the cross section of the specimens.

$$\sigma_{eq} = \sigma_{DIW} V_{DIW} + \sigma_{FFF}(1 - V_{DIW}) \quad (2)$$

3.2 Observations

UTS tests have been made on bone-type specimens for the four kinds of specimen and a synthesis of the results is shown in Fig. 7. All the curves represent the most representative specimen for a given type, i.e. the first specimen having the nearest UTS from the average UTS. In this figure, the average UTS for IM is 59 MPa while FFF technique got an average UTS only at 27 MPa. The specimens type (b), with the three different cross-section 22.5, 45 and 67.5 mm^2 do not exceed the average UTS of specimen (a). Moreover, the prediction of the UTS of the specimens type (b) should have been around 45 MPa based on the Eq. 2 but is only around 15 MPa. One can conclude that the specimen type (b) does not improve the mechanical properties and that a mixing law is not suitable to predict the UTS of such a composite part.

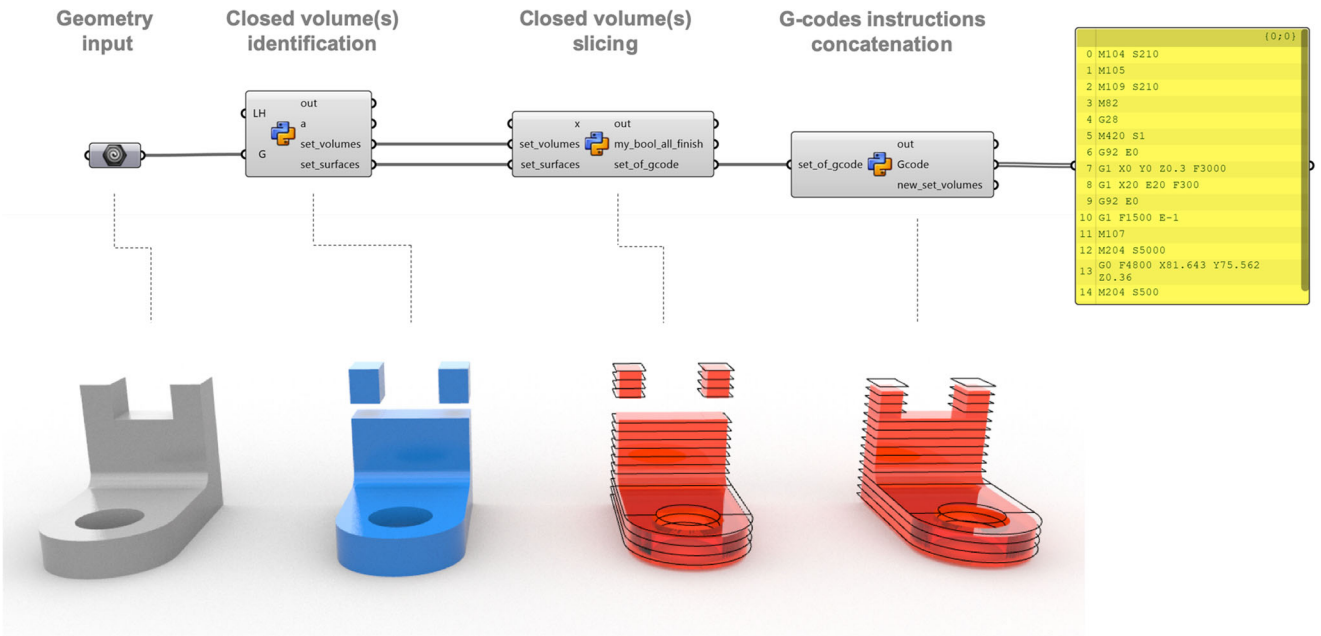

Fig. 5 Digital worflow within Rhinoceros 3D environment and its dedicated visual programming plugin Grasshopper

Table 1 FFF and DIW materials used for specimens realization

AM techniques	a	b	c
FFF	PLA Ariane Plast 4043D	PLA Ariane Plast 4043D	PVA Innofil
DIW	None	Greenpoxy SD56 and hardener 7561	Greenpoxy SD56 and hardener 7561

In contrary, one may observe that the specimen type (c) has a very similar behavior than IM specimen with an average UTS at 52 MPa. The Young modulus is also very close and the relative error of the UTS is inferior to 12% against 47% for specimen type (a). As for the specimen type (c), the mechanical behavior seems to fit with the mechanical behavior of IM parts.

The experiment has been replicated with two other PLA filaments (Ultimaker and Dailyfil) by considering the same epoxy resin. Similar mechanical behavior has been observed: specimens type (b) always have a lower UTS compared to specimens type (a). The UTS observed for those tests are respectively 23.7 MPa (specimens (a) with Ultimaker filament) and 35,5 MPa (specimens (b) with the Dailyfil filament).

3.3 Discussions

Beyond the aforementioned observations, it is important to note that, for an appropriate deposition of the already mixed resin with DIW dispenser, the life pot for the resin needs to be superior to the printing time of the FFF printed part. If this is not the case, the platform could not perform the resin extrusion and this operation will need to be done manually. For such a strategy, the use of a mass casting resin is recommended. By upgrading the proposed hybrid 3D printer with a double syringe and a static mixer, much bigger part can be printed without human intervention on condition that a purge is set up in order to keep the mix into the static mixer soft. As a consequence with such manufacturing strategy, any kind of resin can be used. Another technical issue is about the possible air bubbles forming within the resin mixture, therefore leading to unexpected 3D printed parts quality in terms of mechanical behavior. More study needs to be done to clarify the influence of these parameters on the mechanical properties of the resultingL part.

4 Conclusion and future work

Current status and challenges regarding mechanical performances of 3D printed parts (with FFF and DIW techniques) have been highlighted in this paper. Built on this, an innovative hybrid AM process and platform combining both techniques has been proposed were previous work combined those technique manually. The designed and realized platform actually consists in depositing resins and filaments in a planned manner so as to print at once parts shells and bodies with better mechanical properties than before. Such innovative 3D printing strategy empowers 3D printers to integrate multiple AM techniques and also multiple materials. Derived from this technique, efforts have been made towards designing and building a hybrid 3D printer with the support of a comprehensive digital workflow with reasoning capabilities. The latter has highlighted needs in computational layers so as to properly define the hybrid process plan to any kind of 3D models. As such, three algorithms have been set up and implemented in Rhinoceros/Grasshopper environment in order to translate any 3D models into

Table 2 Applied FFF parameters for specimens

Process parameters	a	b	c
Layer height (mm)	0.2	0.2	0.2
Beads' width (mm)	0.4	0.4	0.4
Printing speed (mm/s)	50	50	20
Extrusion temperature (°C)	205	205	200
Heated bed temperature (° C)	50	50	50

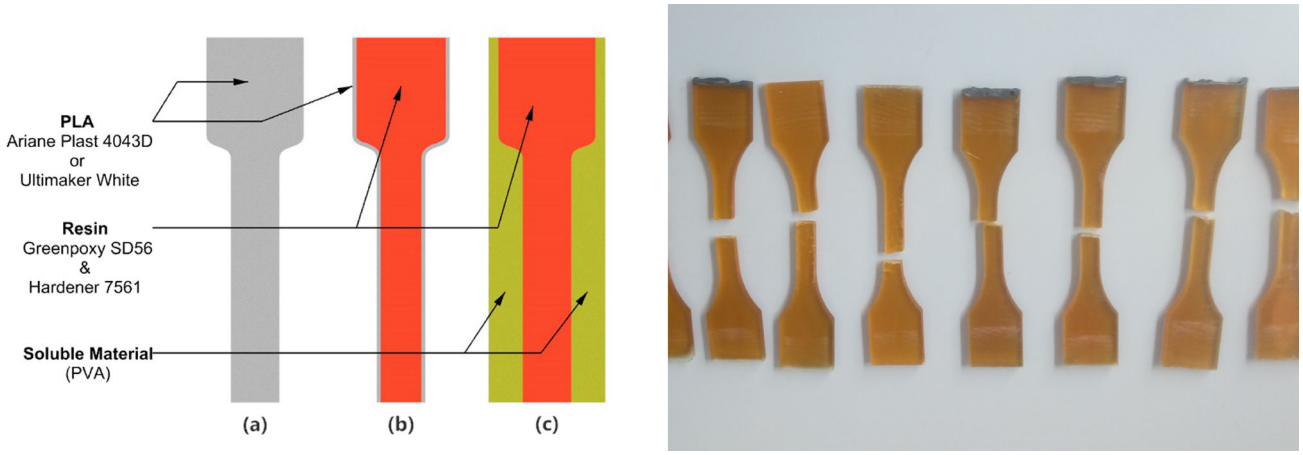

(1) Specimens made according to the three AM strategies (a) Only FFF, (b) hybrid FFF/DiW for shell/infill printing and (c) sacrificial FFF mold/DiW infill

(2) Example of the printed resin specimens related to (c) strategy

Fig. 6 (1) Designed specimens and (2) printed specimens according to the (c) AM strategies and

G-code instructions. The above idea and implementation have been developed and demonstrated through an experimentation and UTS-based evaluation, which have highlighted the relevance of such a strategy to build multi-material parts with enhanced mechanical performances. As short-term perspective, future work will focus on the platform improvement by optimizing the way the resin is handled to open the system to different kinds of resin. The proposed process planning will also be improved to enhance thelb quality of the built parts. A model to predict the mechanical properties of the built part could also be interesting.

Beyond such efforts, the proposed platform seems to be open enough and suitable to pave the way for future research and development in the booming research area of 4D printing. As this emerging paradigm requires AM techniques with multi-material deposition capabilities, future research efforts will be dedicated to address smart materials deposition in conjunction with structural and sacrificial materials. In such a context, the decomposition of a volume into sub-regions will be investigated in order to fulfil the requirement of smart material manufacturing.

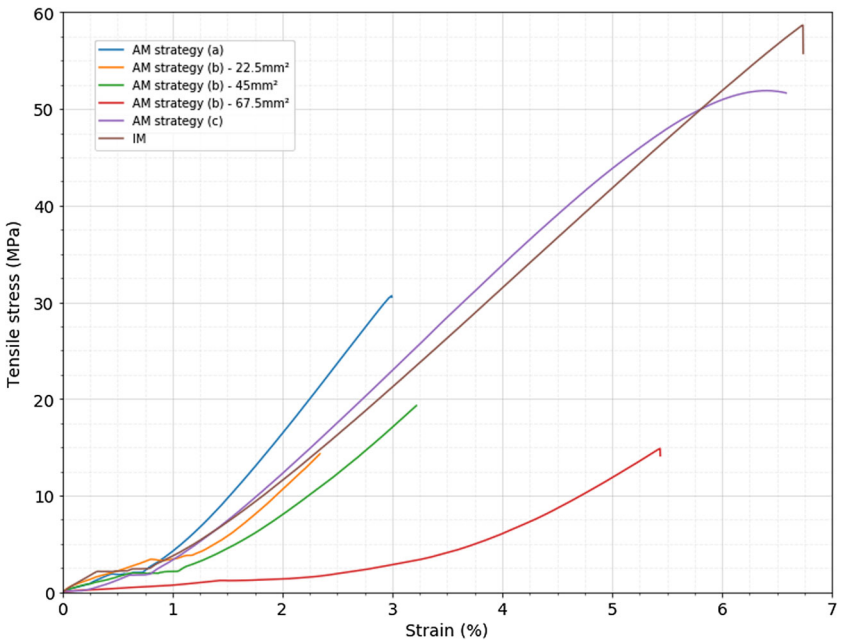

Fig. 7 Synthesis of the UTS related to the 3D printed specimens

Appendix

Table 3 Hybrid 3D printer's bill of materials

Structure	Part ID	Part Name	Quantity	Material
Frame	1	30 mm profile 500 mm	8	Aluminium
	2	30 mm profile 520 mm	4	Aluminium
	3	5mm Panel, 560 * 580 mm	2	PMMA
	4	Corner bracket 30x60mm	24	PLA
Y axis	5	Rod 8 mm diameter - 436mm	4	Steel
	6	Bed wood panel 5mm - 220x220 mm	1	Wood
	7	Heated bed	1	Other
	8	Nema 17	1	Other
	9	Enstop	1	Other
	10	SCS8UU	4	Other
	11	Y front interface	1	PLA
	12	Y back interface	1	PLA
	13	Bed male interface	2	PLA
	14	Bed female interface	2	PLA
	15	Ball bearing F623zz	2	Steel
	16	Belt GT2 - 6mm	1	Rubber
	21	16 teeth pulleys	1	Aluminium
Z axis	8	Nema 17	2	Other
	9	Enstop	2	Other
	17	Rod 8 mm diameter - 380 mm	4	Steel
	18	Jaw shaft coupler 5x8mm	2	Aluminium
	19	SHF8	4	Aluminium
	20	Z endstop holder	2	PLA
	49	KFL08 ball bearings	2	Other
	55	Lead screw - 345 mm	2	Lead
X axis	8	Nema 17	2	Other
	9	Enstop	4	Other
	10	SCS8UU	1	Rubber
	16	Belt GT2 - 6mm	2	Aluminium
	17	Rod 8 mm diameter - 380mm	2	Other
	21	16 teeth pulleys	2	Aluminium
	22	GT2 driven pulley - no teeth	1	Aluminium
	23	XZ interface left	1	PLA
	24	XZ interface right	1	PLA
	37	Lead screw nut	2	Brass
FFF Module	8	Nema 17	4	Other
	10	SCS8UU	2	Other
	25	MK8 extruder	2	Other
	26	MK8 interface	8	PLA
	28	Spool holder male part	4	PLA
	27	Ball bearing 608zz	4	Steel
	29	Spool holder female part	1	PLA
	30	X sliding interface	1	PLA
	31	X belt interface	1	PLA

Table 3 (continued)

Structure	Part ID	Part Name	Quantity	Material
	32	X chimera interface	1	PLA
	33	X enstop pusher	1	PLA
	34	Chimera 3D printer's head	1	Other
DiW Module	8	Nema 17	1	Other
	9	Enstop	4	Other
	10	SCS8UU	1	Other
	17	Rod 8 mm diameter - 380mm	1	Steel
	18	Jaw shaft coupler 5x8mm	1	Aluminium
	27	Ball bearing 608zz	1	Steel
	30	X sliding interface	1	PLA
	31	X belt interface	1	PLA
	33	X enstop pusher	1	PLA
	35	Tube's interface	2	PLA
	36	Lead screw - 200 mm	1	Lead
	37	Lead screw nut	2	Brass
	38	Threaded shaft M8 - 400mm	1	Steel
	39	DIW structure interface	1	PLA
	40	DIW rotational arm	1	PLA
	41	DIW Top interface	1	PLA
	42	DIW Syringe interface	1	PLA
	43	DIW Bottom interface	1	PLA
	44	Piston	2	PLA
	45	DIW Nut interface	1	PLA
	46	DIW endstop interface	1	PLA
	47	30cc syringe	1	Polypropylene
	48	Syringe tip	1	Polypropylene
Electronic	50	Arduino 2560 Rev 3	1	Other
	51	RepRap Smart controller	1	Other
	52	Ramps 1.4	1	Other
	53	Stepper expander	3	Other
	54	12V DC power supply	1	Other

Acknowledgements The research activity has been made in collaboration with Segula company as part of a CIFRE contract (Industrial Standards of Research Training) by the French National Agency for Research Agency for Research and Technology (ANRT) in conjunction with the French "Investissements d'Avenir" program, project ISITE-BFC (contract ANR-15-IDEX-0003). The authors would like to thank all financial supports and also Dr. Lachat (ICB lab) for his valuable assistance in realizing the specimens.

Author Contributions Thibaut Cadiou: conceptualization; methodology; software; writing original draft. Frédéric Demoly: conceptualization; methodology; writing—review and editing; supervision. Samuel Gomes: funding acquisition; supervision.

Funding The research work was funded by the French National Agency for Research Agency for Research and Technology (ANRT) in conjunction with the French "Investissements d'Avenir" program, project ISITE-BFC (contract ANR-15-IDEX-0003).

Declarations

Consent to participate The authors are consent to participate.

Consent for publication The authors are consent for publication.

Conflict of interests The authors declare no competing interests.

References

1. Wohlers T, Gornet T (2016) History of additive manufacturing. Wolhers Report 38
2. Jiang J, Newman ST, Zhong RAYY (2021) A review of multiple degrees of freedom for additive manufacturing machines. Int J Comput Integr Manuf 34(2):195–211

3. Jingchao J, Yongsheng M (2020) Path planning strategies to optimize accuracy, quality, build time and material use in additive manufacturing: a review . Micromachines 11(7):633
4. Lay M, Thajudin NLN, Hamid ZAA, Rusli A, Abdullah MK, Shuib RK (2019) Comparison of physical and mechanical properties of PLA, ABS and nylon 6 fabricated using fused deposition modeling and injection molding. Compos B Eng 176:107341
5. Jiang J (2020) A novel fabrication strategy for additive manufacturing processes. J Clean Prod 272:122916
6. Jiang Jingchao, Yun-Fei Fu (2020) A short survey of sustainable material extrusion additive manufacturing. Aust J Mech Eng 1–10
7. Ahn SH, Montero M, Odell D, Roundy S, Wright PK (2002) Anisotropic material properties of fused deposition modeling ABS. Rapid Prototyp. J. 8(4):248–257
8. Rajpurohit SR, Dave HK (2018) Effect of process parameters on tensile strength of FDM printed PLA part. Rapid Prototyp J 24(8):1317–1324
9. Jones R, Haufe P, Sells E, Iravani P, Olliver V, Palmer C, Bowyer A (2011) RepRap – the replicating rapid prototyper. Robotica 29(01):177–191
10. Cisneros-López EO, Pal AK, Rodriguez AU, Wu F, Misra M, Mielewski DF, Kiziltas A, Mohanty AK (2019) Recycled poly(lactic acid)–based 3D printed sustainable biocomposites: a comparative study with injection molding. Materials Today Sustainability 7–8:100027
11. Dawoud M, Taha I, Samy JE (2016) Mechanical behaviour of ABS An experimental study using FDM and injection moulding techniques. J Manuf Process 21:39–45
12. McLouth TD, Severino JV, Adams PM, Patel DN, Zaldivar RJ (2017) The impact of print orientation and raster pattern on fracture toughness in additively manufactured ABS. Addit Manuf 18:103–109
13. Zhang Y, Chou YK (2006) Three-dimensional finite element analysis simulations of the fused deposition modelling process. Proc Inst Mech Eng Part B J Eng Manuf 220(10):1663–1671
14. Garzon-Hernandez S, Garcia-Gonzalez D, Jérusalem A, Arias A (2020) Design of FDM 3D printed polymers: an experimental-modelling methodology for the prediction of mechanical properties. Mater Des 108414:188
15. Alaimo G, Marconi S, Luca C, Ferdinando A (2017) Influence of meso-structure and chemical composition on FDM 3D-printed parts. Compos B Eng 113:371–380
16. Li H, Wang T, Li Q, Zhiqiang Y, Na W (2018) A quantitative investigation of distortion of polylactic acid/PLA) part in FDM from the point of interface residual stress. Int J Adv Manuf Technol 94(1-4):381–395
17. Martínez J, Diéguez JL, Ares E, Pereira A, Hernández P, Pérez JA (2013) Comparative between FEM Models for FDM Parts and their Approach to a Real Mechanical Behaviour. Procedia Eng 63:878–884
18. Zhao Y, Yuansong Chen, Yongjun Zhou (2019) Novel mechanical models of tensile strength and elastic property of FDM AM PLA materials: experimental and theoretical analyses. Mater Des 181:108089
19. Zaldivar RJ, McLouth TD, Patel DN, Severino JV, Kim HI (2017) Strengthening of plasma treated 3D printed ABS through epoxy infiltration. Prog Addit Manuf 2(4):193–200
20. Klar V, Pearce JM, Kärki P, Ystruder PK (2019) Open source multifunction extruder with sensing and monitoring capabilities. HardwareX 6:e00080
21. Lipton JI, Cohen D, Heinz M, Lobovsky M, Parad W, Bernstein G, Li T, Quartiere J, Washington K, Umaru A-A, Masanoff R, Granstein J, Whitney J, Hod Lipson (2019) Fab@Home Model 2: towards ubiquitous personal fabrication devices. Solid Freeform Fabrication 12
22. Wang G, Yao L, Wang W, Jifei O, Cheng C-Y, Hiroshi I (2016) xPrint: A modularized liquid printer for smart materials deposition. In: Proceedings of the 2016 CHI conference on human factors in computing systems, CHI '16, pages 5743–5752, San Jose, California, USA, Association for Computing Machinery
23. Górski F, Wichniarek R, Kuczko W (2014) Influence of filling type on strength of parts manufactured by Fused Deposition Modelling. J Mach Eng 14(3):113–125
24. Belter JT, Aaron MD (2015) Strengthening of 3D Printed Fused Deposition Manufactured Parts Using the Fill Compositing Technique. PLoS One 10(4):4–6
25. Matos MA, Rocha AMAC, Pereira ANAI (2019) On optimizing the build orientation problem using genetic algorithm. AIP Conference Proceedings 220006
26. https://www.nanowerk.com (2019)
27. https://www.matterhackers.com (2020)
28. https://e3d-online.com/chimera (2019)
29. https://reprap.org/wiki/RepRapDiscount_Smart_Controller (2019)
30. https://marlinfw.org/docs/basics/introduction.html (2019)
31. https://www.arianeplast.com/pla-format-1-kg/104-pla-blanc-4043d-1kg.html (2019)

Publisher's note Springer Nature remains neutral with regard to jurisdictional claims in published maps and institutional affiliations.